

$3d$ $\mathcal{N} = 4$ Quiver Gauge Theory and Mirror Symmetry



Leyi Jiang
Lady Margaret Hall
University of Oxford

A dissertation submitted for the degree of
MMath in Mathematics

Trinity 2025

Acknowledgements

I would first and foremost like to express my deepest gratitude to my supervisor, Dr. Zhenghao Zhong. It was through his guidance that I was introduced to the fascinating world of quiver gauge theory. I am incredibly thankful for his concise and insightful answers to my many questions and for the constant enthusiasm and positive energy he brought to our meetings, which were always motivating. His support has been invaluable throughout this project.

I would also like to extend my sincere thanks to my peers, Jazz Ooi and Richard Stone. Our discussions were always stimulating, and they were invaluable for discussing ideas and working through challenges.

My journey through my undergraduate years at Oxford has been enriched by so many wonderful people. I am deeply grateful to my friends for their unwavering support and camaraderie. Special thanks go to Bangye Wu and Xingzhe Li for proofreading my drafts and for providing invaluable feedback from an outside perspective, which greatly improved the clarity of this work. I also owe a debt of gratitude to my tutors at Lady Margaret Hall – Rolf Suabedissen, Christina Goldschmidt, Jochen Koenigsmann, Michael Monoyios, and William Hart – for their guidance and academic support throughout my studies. A heartfelt thank you to the Oxford PhoenOx Chinese Dance Society, and everyone I have met there; it has been a true source of belonging and a cherished refuge when I needed it most. Finally, to my boyfriend, Huanxing Chen, thank you for your constant love, support, and for always being by my side through every challenge and triumph.

Last but not least, I wish to express my deepest gratitude to my family for their unwavering support, understanding, and encouragement throughout my life.

Contents

1	Introduction	1
2	Background	3
2.1	Quantum Field Theory	3
2.2	Supersymmetry	3
2.2.1	$3d \mathcal{N} = 4$ Supersymmetry Theory	4
2.2.2	Supermultiplets	4
2.3	Moduli Space of Vacua	5
2.4	Quiver Gauge Theory	6
3	Hilbert Series, Coulomb and Higgs Branch	8
3.1	More on the moduli space	8
3.2	Hilbert Series	9
3.2.1	Monopole Formula	10
3.2.2	Molien-Weyl Formula	12
3.3	Mirror Symmetry	14
4	Brane Dynamics	15
4.1	Branes	15
4.2	Quiver Theories and Branes	17
4.3	$3d$ Mirror Symmetry and Branes	17
5	Non-linear Quivers	20
5.1	The Postulate	21
5.2	Essential Tools: Quiver Operations	22
5.3	Verification of the Postulate	25
5.3.1	Base Case Verification via Hilbert Series	25
5.3.2	Inductive Argument	26

Bibliography	29
A Hilbert Series Verification for Base Cases	30
B Hilbert Series Computations for $n = 4$	31

List of Figures

4.1	An example of $3d$ mirror symmetry construction via brane setups. . .	19
5.1	The $3d$ mirror pairs Theory $Q = Q_{[n; \{g_i\}; \{l_i\}]}$ and Theory $P = P_{[n; \{g_i\}; \{l_i\}]}$	21
5.2	Fixing or removing a centre of mass preserves the moduli space . . .	22
5.3	Flavour-Gauged Linking operation (left) and its corresponding mirror operation (right)	24
5.4	Brane setup of a general linear rank-1 quiver under Flavour-Gauged Linking operation	24
5.5	Proof by induction on parametre l_1	27
5.6	Proof by induction on parametre g_n	27

Chapter 1

Introduction

$3d$ Mirror Symmetry is a special yet important duality within the study of $3d \mathcal{N} = 4$ supersymmetric quiver gauge theories. Its power lies in relating pairs of distinct quiver theories through an isomorphism that exchanges their Coulomb and Higgs branches. This duality offers significant insight into the structure of theories and computational advantages.

Despite its utility, the systematic understanding and application of $3d$ mirror symmetry, particularly its derivation via brane dynamics, have largely been confined to theories represented by relatively simple quiver diagrams, such as linear chains or those of ADE type. A compelling open area is the exploration of how this duality manifests in theories characterised by more intricate, non-linear quiver structures. Developing a deeper understanding of these less-explored regimes is essential for a comprehensive grasp of the landscape of $3d \mathcal{N} = 4$ theories.

This dissertation is directly motivated by the challenge of extending the scope of known $3d$ mirror symmetry dualities. The core aim is to propose and rigorously investigate a novel infinite family of conjectured mirror pairs. These pairs feature Abelian gauge theories whose quivers involve non-linear, branched cyclic structures, venturing beyond the well-trodden territory of linear and ADE geometries. By examining this new family, this work seeks to uncover fundamental principles governing mirror symmetry in more complex settings, potentially providing insights applicable to even broader classes of quiver theories.

The thesis is structured as follows:

- **Chapter 2: Background** reviews the foundational concepts required, including Quantum Field Theory, supersymmetry (focusing on $3d \mathcal{N} = 4$), the structure of supermultiplets, the moduli space of vacua, and the formalism of quiver gauge theories.

- **Chapter 3: Hilbert Series, Coulomb and Higgs Branch** delves into the properties of the moduli space, introducing the Hilbert Series as a tool for characterising different quivers. It details the Monopole Formula for the Coulomb branch and the Molien-Weyl formula for the Higgs branch, and formally defines $3d$ mirror symmetry.
- **Chapter 4: Brane Dynamics** explains how $3d \mathcal{N} = 4$ quiver theories and their mirror symmetries can be engineered using specific D3-D5-NS5 brane configurations in Type IIB string theory, including the S-duality transformation that realises mirror symmetry.
- **Chapter 5: Non-linear Quivers** presents the central, original contribution of this work. It postulates the new infinite family of mirror dual pairs. Evidence for this postulate is provided through Hilbert Series computations for base cases and a detailed inductive argument based on specific quiver operations and their mirror counterparts. Consistency with known results for $n = 3$ is discussed.

Chapter 2

Background

2.1 Quantum Field Theory

Quantum Field Theory (QFT) is a theoretical framework that integrates Quantum Theory and Special Relativity, describing particle interactions through fields that permeate spacetime, where particles are modelled as perturbations of their associated underlying quantum fields.

However, as the richness of the field content increases, the task of merely formulating the appropriate Lagrangian, which encapsulates the dynamics of the system, can present considerable difficulty, often necessitating sophisticated techniques to manage the resultant quantum corrections.

2.2 Supersymmetry

Supersymmetry emerges as a theoretical principle imposing highly useful constraints upon quantum field theories, frequently endowing them with elegant mathematical properties. It significantly enhances the tractability of QFT analyses and computations, making them more mathematically manageable. This postulate not only offers the potential for a more consistent and unified description of nature but has also proven instrumental in uncovering deep connections between quantum field theory and disparate areas of mathematics, such as algebraic geometry, as well as other domains of theoretical physics, notably string theory.

The supercharge, denoted as Q , is a fundamental concept in supersymmetric theories, acting as the generator of supersymmetry transformations. It transforms bosonic states into fermionic states and vice versa. The number of independent real supercharges a theory possesses is a measure of its supersymmetry; a higher number of su-

percharges implies a more symmetric theory, which in turn imposes more constraints on the theory's structure.

2.2.1 $3d \mathcal{N} = 4$ Supersymmetry Theory

This dissertation will focus on a specific case of supersymmetry, namely the $3d \mathcal{N} = 4$ theories. The theory takes place in a space with two spatial dimensions and one time dimension. The parameter \mathcal{N} counts the number of sets of supercharges present in the theory, with $\mathcal{N} = 4$ indicating the existence of four distinct sets of supercharges. Each minimal spinor representation in $3d$ is real and consists of two components. Therefore, a $3d \mathcal{N} = 4$ theory incorporates four minimal spinor sets, which are equal to eight supercharges in total.

This setup is analogous to $4d \mathcal{N} = 2$ theories, where the minimal Weyl spinor comprises two complex components (equivalently, four real components). The $\mathcal{N} = 4$ theory in $3d$ is of particular interest in string theory, where it can emerge from specific brane configurations, which will be covered in Chapter 4.

The spacetime symmetry of this theory is governed by the Lorentz group $SU(2)$, and its R -symmetry group is $SO(4)$, which describes rotations in four dimensions and has six generators. Notably, $SO(4)$ is locally isomorphic to $SU(2) \times SU(2)$, often represented in the physics context as

$$SU(2) = SU(2)_L \times SU(2)_R. \quad (2.1)$$

2.2.2 Supermultiplets

Supermultiplets constitute the representations of the supersymmetry algebra. Formally, a supermultiplet comprises a collection of particles, or equivalently fields, which are related to one another through the action of supersymmetry transformations. The constituent particles belonging to a specific supermultiplet transform into each other under the operation of the supercharges. Within the context of $3d \mathcal{N} = 4$ supersymmetry, two fundamental types of irreducible supermultiplets, which cannot be decomposed into smaller representations of the supersymmetry algebra, are of primary importance: **vector multiplets** and **hypermultiplets**.

Vector multiplets represent a class of supermultiplets primarily characterised by the presence of a gauge field (a vector boson) amongst their components. In addition to the gauge field, these multiplets necessarily contain associated superpartners, including fermions and scalar fields. Specifically, in three-dimensional $\mathcal{N} = 4$ theories, a vector multiplet includes a gauge field A_μ (where $\mu = 1, 2, 3$), three real

scalar fields denoted $\phi_i^V, i = 1, 2, 3$, and accompanying spinors. With respect to the $SO(4) \simeq SU(2)_L \times SU(2)_R$ R-symmetry, the scalar fields ϕ_i^V transform non-trivially under the adjoint representation of the $SU(2)_L$ factor, while remaining invariant under $SU(2)_R$.

Hypermultiplets constitute the second fundamental type of irreducible supermultiplet, typically representing the matter fields of the theory. For $3d \mathcal{N} = 4$ supersymmetry, a hypermultiplet contains two complex scalar fields, collectively denoted ϕ^H (equivalent to four real scalar degrees of freedom), along with associated spinor fields. In contrast to the scalars in the vector multiplet, the hypermultiplet scalars ϕ^H transform non-trivially under the $SU(2)_R$ factor of the R-symmetry group.

2.3 Moduli Space of Vacua

In the context of quantum field theory, a “vacuum” (plural: vacua) signifies a state corresponding to the lowest possible energy configuration, representing the ground state of the theory. The vacuum state holds foundational importance because it constitutes the background spacetime from which particle excitations and perturbations emerge. A characteristic feature of many supersymmetric theories is the absence of a unique vacuum; instead, owing to the constraints imposed by supersymmetry, there often exists a continuous family of states possessing the same minimal energy. The geometric space parametrising this continuum of possible ground states is referred to as the moduli space of vacua. In scenarios where supersymmetry remains unbroken, this minimal energy is precisely zero. A specific vacuum configuration within this space is characterised by the constant values acquired by the scalar fields present in the theory; these constant values are known as Vacuum Expectation Values (VEVs).

The dynamics and properties of a quantum field theory, including its field content, kinetic terms, mass parameters, interactions, and symmetries, are comprehensively encoded within its Lagrangian density, often referred to simply as the Lagrangian. A crucial component of the Lagrangian for theories containing scalar fields is the scalar potential, denoted $V(\phi^V, \phi^H)$, which is a function solely of the scalar fields (here schematically separated into vector multiplet scalars ϕ^V and hypermultiplet scalars ϕ^H). This potential term dictates the energy associated with any given configuration of these scalar fields. For a vacuum state to preserve supersymmetry, the scalar potential must vanish. Consequently, the identification of supersymmetric vacua is mathematically equivalent to finding the solutions to the equation $V(\phi^V, \phi^H) = 0$; this is known as the vacuum condition.

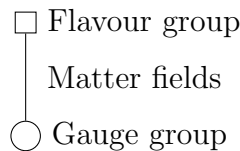
The vacuum condition typically manifests as a system of polynomial equations involving the scalar field VEVs. From a mathematical perspective, the set of common solutions to such a system of polynomial equations defines a geometric object known as an algebraic variety.

Therefore, the moduli space of vacua can be understood as an algebraic variety. Each point residing on this variety corresponds to a permissible set of VEVs that satisfy the vacuum condition, thereby representing a distinct vacuum state of the theory. Algebraic varieties possess associated generating functions that encode structural information; notable among these is the Hilbert Series, which will be our main focus in the next Chapter.

2.4 Quiver Gauge Theory

Quiver gauge theories offer a particularly clear and intuitive visual representation for describing the structure of gauge theories, including their field content and interactions, which can often be quite complex. The specific graphical conventions employed in quiver diagrams may vary depending on the amount of supersymmetry the theory possesses. For theories with eight supercharges, such as the $3d \mathcal{N} = 4$ theories, the quiver diagram is typically depicted as an undirected graph. This graph consists of several key components:

- Circular nodes represent the gauge groups of the theory;
- Square nodes represent the flavour symmetry groups; and
- Edges connecting these nodes represent matter fields.



While the gauge groups can belong to various families, including unitary, special unitary, orthogonal, or symplectic groups, the focus herein will be restricted primarily to unitary groups $U(N_c)$, where N_c is the rank of the group, often referred to as the number of “colours”. Similarly, flavour groups are typically $S(U(N_f))$, with N_f representing the number of “flavours”.

In the context of supersymmetry, matter fields are packaged into supermultiplets. For theories with eight supercharges, the matter fields associated with quiver edges

are typically hypermultiplets. Moreover, vector multiplets associated with gauge nodes invariably transform in the adjoint representation of their respective gauge group, while hypermultiplets corresponding to edges transform in the bifundamental representation of the groups associated with the two nodes (either gauge or flavour) that the edge connects.

More examples of quivers will be presented in the upcoming chapters of this paper.

Chapter 3

Hilbert Series, Coulomb and Higgs Branch

Building directly upon this foundation of QFT introduced in Chapter 2, this chapter delves into a more quantitative characterisation of the moduli space in $3d \mathcal{N} = 4$ theories. We will first examine two important subsets of the moduli space, the Coulomb and Higgs branches. A central focus will then be the introduction of the Hilbert Series, a powerful generating function that provides precise information about the algebraic geometry of these branches. We will subsequently explore specific techniques for computing the Hilbert Series for both the Coulomb branch (via the Monopole Formula) and the Higgs branch (via the Molien-Weyl Formula). Finally, equipped with these tools, we will introduce the profound concept of $3d$ Mirror Symmetry, a duality that intricately connects these moduli space structures across seemingly different theories.

3.1 More on the moduli space

The moduli space \mathcal{M} of a given theory parametrizes the set of possible vacuum states, denoted $|\alpha\rangle$. Each such vacuum state is characterized by the vacuum expectation values, S_α , acquired by the scalar fields $s(x)$ of the theory, formally defined as

$$S_\alpha = \langle \alpha | s(x) | \alpha \rangle. \quad (3.1)$$

Within the moduli space, distinct subsets, often called branches, are typically identified based on which specific types of scalar fields acquire non-zero VEVs.

Two principal branches are commonly distinguished:

- **Coulomb Branch (\mathcal{M}_C):** This subspace consists of vacuum configurations wherein only the scalar fields originating from vector multiplets, denoted ϕ^V ,

possess non-trivial VEVs. Conversely, scalar fields belonging to hypermultiplets are constrained to have vanishing VEVs ($\phi^H = 0$). The Coulomb branch is thus defined by the solutions to the vacuum condition

$$V(\phi^V, \phi^H = 0) = 0. \quad (3.2)$$

- **Higgs Branch (\mathcal{M}_H):** This subspace encompasses vacuum states where the only scalar fields acquiring non-zero VEVs are those associated with hypermultiplets, ϕ^H . Correspondingly, the scalar components of vector multiplets are set to zero ($\phi^V = 0$). The Higgs branch is therefore determined by the solutions to the vacuum condition

$$V(\phi^V = 0, \phi^H) = 0. \quad (3.3)$$

In addition to these two primary branches, the full moduli space \mathcal{M} may also contain mixed branches (\mathcal{M}_I), characterized by non-zero VEVs for scalars from both vector and hypermultiplets. Generically, the Coulomb and Higgs branches intersect only at the origin of the moduli space, corresponding to the point where all scalar VEVs vanish ($\phi^V = 0, \phi^H = 0$), and the full gauge symmetry of the theory is restored.

For theories endowed with eight supercharges, the moduli space is decomposed into Coulomb, Higgs, and potentially mixed branches, and they exhibit distinct behaviours under quantum effects. The Coulomb branch is known to receive significant quantum corrections, therefore can be very difficult to calculate. In contrast, the Higgs branch is protected from quantum corrections by non-renormalization theorems.[2] Consequently, the structure of the Higgs branch can typically be computed using classical or semi-classical methods, such as the hyperKähler quotient construction, directly from the Lagrangian specification of the theory.

3.2 Hilbert Series

The Hilbert series (HS) serves as a powerful analytical tool in the study of moduli spaces in supersymmetric gauge theories. When the moduli space is regarded as an algebraic variety, the Hilbert series functions as a generating function that enumerates the dimensions of spaces of linearly independent holomorphic functions, graded by degree. Specifically, when expressed as a Taylor expansion in a fugacity t ,

$$HS(t) = \sum_{d=0}^{\infty} m_d t^d, \quad (3.4)$$

the coefficient m_d quantifies the number of linearly independent homogeneous polynomials of degree d within the coordinate ring of the variety.

Alternatively, viewing the moduli space through the lens of the associated ring of chiral operators, the Hilbert series counts gauge-invariant chiral operators, graded according to their conformal dimensions. Consequently, the Hilbert series provides significant insights into both the geometric structure of the moduli space and the algebraic properties of its associated chiral ring.

Next, I will introduce how we can compute the Hilbert series for both the Coulomb and Higgs branches.

3.2.1 Monopole Formula

Analysing the Coulomb branch of supersymmetric gauge theories presents significant challenges, primarily due to the influence of quantum corrections. The monopole formula [4] offers a systematic method to compute the Hilbert series of the Coulomb branch.

The monopole formula, for a theory with gauge group G , is a function in t , the counting fugacity,

$$\text{HS}_{\text{Coulomb}}(t) = \sum_{m \in \Gamma_{G^\vee}/W_{G^\vee}} t^{2\Delta(m)} P_G(t, m), \quad (3.5)$$

Where the Hilbert series is a sum over magnetic charge configurations m . These magnetic charges m are drawn from the charge lattice given by $\Gamma_{G^\vee}/W_{G^\vee}$, where Γ_{G^\vee} is the weight lattice of the GNO dual group of the gauge group G , and W_{G^\vee} is the Weyl group of G . The exponent $\Delta(m)$ represents the conformal dimension, or R-charge, of the bare monopole operator associated with magnetic charge m . Its value is determined by the theory's field content, specifically, with N_f hypermultiplets in the representation \mathcal{R}_i :

$$\Delta(m) = - \sum_{\alpha \in \Delta_+} |\alpha(m)| + \frac{1}{2} \sum_{i=1}^{N_f} \sum_{\rho \in \mathcal{R}_i} |\rho_i(m)|, \quad (3.6)$$

where α are the positive roots of the algebra $\mathfrak{g} = \text{Lie}(G)$. The first term is contributions from the vector multiplets transforming in the adjoint representation G , while the second term is the contributions from N_f hypermultiplets transforming in representation R_i with weights ρ . Finally, the dressing factor P_G takes the form

$$P_G(m, t) = \prod_{i=1}^{\text{rank}(G)} \frac{1}{1 - t^{2d_i(m)}}, \quad (3.7)$$

where $d_i(m)$ is the Casimir invariant of G .

For some specific gauge groups commonly encountered in quiver theories, the structure of the magnetic charges m entering the monopole formula is well-defined. For a unitary gauge group $U(k)$ of rank k , the magnetic charge $m = (m_1, m_2, \dots, m_k)$ consists of integer components $m_i \in \mathbb{Z}$, satisfying

$$\infty > m_1 \geq m_2 \geq \dots \geq m_k > -\infty. \quad (3.8)$$

The conformal dimension $\Delta(m)$ encodes structural information about the quiver interactions. For instance, the contribution arising purely from the $U(k)$ vector multiplet interactions is given by:

$$\Delta(U(k)) = - \sum_{1 \leq i < j \leq k} |m_i - m_j|, \quad (3.9)$$

and $\Delta = 0$ for $k = 1$. The interaction between two gauge groups $U(k_1)$ and $U(k_2)$ mediated by a bifundamental hypermultiplet contributes:

$$\Delta(U(k_1) - U(k_2)) = \frac{1}{2} \sum_{i=1}^{k_1} \sum_{j=1}^{k_2} |m_i - n_j|. \quad (3.10)$$

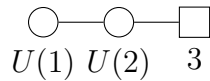
Finally, N_f fundamental hypermultiplets coupled to a $U(k)$ gauge group contribute:

$$\Delta(U(k) - N_f) = \frac{N_f}{2} \sum_{i=1}^k |m_i|. \quad (3.11)$$

The dressing factor $P_G^v(t, m)$, representing contributions from Casimir invariants preserved by the magnetic charge m , also depends on the structure of the gauge group and the specific charge m . As an example, consider a $U(3)$ gauge group where the magnetic charge $m = (3, 3, 1)$ breaks the symmetry to $U(2) \times U(1)$. The corresponding dressing factor is given by:

$$P_{U(3)}(m, t) = \frac{1}{(1-t^2)(1-t^4)(1-t^2)}. \quad (3.12)$$

Now, to provide a concrete application, consider the linear quiver gauge theory represented by



corresponding to $U(1) \times U(2)$ gauge groups with the $U(2)$ node coupled to $N_f = 3$ fundamental flavours, associated with an $SU(3)$ flavour symmetry. Magnetic charges are $a_1 \in \mathbb{Z}$ for the $U(1)$ factor and $(b_1, b_2) \in \mathbb{Z}^2$ with $b_1 \geq b_2$ for the $U(2)$ factor. Applying the component formulae for Δ , the conformal dimension for a general magnetic charge (a_1, b_1, b_2) is:

$$\Delta(a_1, b_1, b_2) = \underbrace{-|b_1 - b_2|}_{\Delta(U(2))} + \underbrace{\frac{1}{2}(|a_1 - b_1| + |a_1 - b_2|)}_{\Delta(U(1)-U(2))} + \underbrace{\frac{3}{2}(|b_1| + |b_2|)}_{\Delta(U(2)-3)}. \quad (3.13)$$

Substituting this dimension and the appropriate dressing factor into the monopole formula yields the Hilbert series for the Coulomb branch:

$$\text{HS}_{\text{Coulomb}}(t) = \sum_{a_1=-\infty}^{\infty} \sum_{b_1=-\infty}^{\infty} \sum_{b_2=-\infty}^{b_1} t^{2\Delta(a_1, b_1, b_2)} P(a_1, b_1, b_2, t). \quad (3.14)$$

Performing the summation, the initial terms of the series expansion are found to be:

$$\text{HS}_{\text{Coulomb}}(t) = 1 + 8t^2 + 35t^4 + 111t^6 + 286t^8 + O(t^{10}). \quad (3.15)$$

3.2.2 Molien-Weyl Formula

While the monopole formula provides a powerful mechanism for computing the Hilbert series of the Coulomb branch, the analysis of the Higgs branch often employs different techniques rooted in invariant theory, specifically the computation of hyperKähler quotients via the Molien-Weyl formula.

A central tool in this approach is the Plethystic Exponential (PE). For a given function or character $f(t_1, t_2, \dots, t_n)$, its plethystic exponential is defined as:

$$PE[f(t_1, t_2, \dots, t_n)] = \exp \left(\sum_{k=1}^{\infty} \frac{f(t_1^k, t_2^k, \dots, t_n^k)}{k} \right). \quad (3.16)$$

To apply this to gauge theories, one typically requires the characters of relevant representations. For instance, the character of a $U(n)$ group element G can be expressed in terms of its eigenvalues (m_1, \dots, m_n) , noting that all $U(n)$ matrices are diagonalisable. The characters for the fundamental and anti-fundamental representations are then given by:

$$\chi_{U(n)}^{\text{fund}} = \text{Tr}(G) = m_1 + \dots + m_n, \quad (3.17)$$

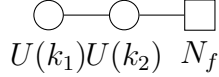
$$\chi_{U(n)}^{\text{anti}} = \text{Tr}(G^{-1}) = \frac{1}{m_1} + \dots + \frac{1}{m_n}. \quad (3.18)$$

The computation of the unrefined Hilbert series for the Higgs branch, HS_{Higgs} , proceeds by considering all possible constant field configurations for the hypermultiplet scalars (compatible with $\phi^V = 0$) and then projecting onto gauge-invariant combinations. This projection is achieved through integration of the gauge group G using the Haar measure $d\mu_G$. The general structure takes the form of the Molien-Weyl integral:

$$HS_{\text{Higgs}} = \oint d\mu_G \frac{PE[\text{character of all constant matter field configurations}]}{PE[\text{character of constraints}]} \quad (3.19)$$

Here, the numerator is refined by fugacity t while the denominator is weighted differently, by t^2 .

As an example, consider the quiver



The matter content consisting of bifundamental hypermultiplets between $U(k_1)$ and $U(k_2)$, and between $U(k_2)$ and the $SU(N_f)$ flavour group. The Higgs branch Hilbert series integral is formulated as:

$$HS_{\text{Higgs}}(t) = \oint d\mu_{U(k_1)} d\mu_{U(k_2)} \frac{PE[\chi_{k_1}^{\text{fund}} \chi_{k_2}^{\text{anti}} + \chi_{k_1}^{\text{anti}} \chi_{k_2}^{\text{fund}} + N_f(\chi_{k_2}^{\text{fund}} + \chi_{k_2}^{\text{anti}}), t]}{PE[\chi_{k_1}^{\text{fund}} \chi_{k_1}^{\text{anti}} + \chi_{k_2}^{\text{fund}} \chi_{k_2}^{\text{anti}}, t^2]}. \quad (3.20)$$

Now, to illustrate the procedure with a concrete example, let us take $k_1 = 1, k_2 = 2$ and $N_f = 3$. Let a_1 be the eigenvalue of $U(1)$ and b_1, b_2 be the eigenvalues of $U(2)$, the Higgs branch Hilbert series is computed as follows:

$$HS_{\text{Higgs}}(t) = \oint d\mu_{U(1)} d\mu_{U(2)} \frac{PE[a_1(\frac{1}{b_1} + \frac{1}{b_2}) + \frac{1}{a_1}(b_1 + b_2) + 3[(b_1 + b_2) + (\frac{1}{b_1} + \frac{1}{b_2})], t]}{PE[a_1 \frac{1}{a_1} + (b_1 + b_2)(\frac{1}{b_1} + \frac{1}{b_2}), t^2]} \quad (3.21)$$

$$= \frac{(1+t^2)(1-t+t^2)(1+t+t^2)}{(-1+t)^6(1+t)^6} \quad (3.22)$$

$$= 1 + 8t^2 + 35t^4 + 111t^6 + 286t^8 + O(t^{10}). \quad (3.23)$$

Comparing 3.21 with 3.15, the resulting Hilbert series expansion for the Higgs and Coulomb branches matches precisely for our example quiver theory. This coincidence is not accidental; it arises because this quiver belongs to a particular family of $3d \mathcal{N} = 4$ quiver gauge theories that are self-mirrored under $3d$ mirror symmetry.

3.3 Mirror Symmetry

Introduced by Intriligator and Seiberg in 1996 [9], $3d$ mirror symmetry is a duality relating pairs of $3d \mathcal{N} = 4$ quiver gauge theories. Specifically, given two such theories, denoted Q_1 and Q_2 , they are said to constitute a $3d$ mirror pair if the Coulomb branch of Q_1 is isomorphic to the Higgs branch of Q_2 , and concurrently, the Higgs branch of Q_1 is isomorphic to the Coulomb branch of Q_2 , i.e.

$$\text{Coulomb}(Q_1) \cong \text{Higgs}(Q_2) \quad \text{and} \quad \text{Higgs}(Q_1) \cong \text{Coulomb}(Q_2). \quad (3.24)$$

This duality proves highly useful in theoretical studies, as properties that may be difficult to compute or analyse in one theory might become significantly simpler when examined within the context of its mirror dual.

Although the Hilbert series, as a generating function, does not possess sufficient power to uniquely identify a given moduli space, it serves as a handy tool and a necessary condition for verifying proposed $3d$ mirror pairs. The isomorphism of mirror symmetry implies that

$$HS_{\text{Coulomb}}^{Q_1}(t) = HS_{\text{Higgs}}^{Q_2}(t) \quad \text{and} \quad HS_{\text{Higgs}}^{Q_1}(t) = HS_{\text{Coulomb}}^{Q_2}(t). \quad (3.25)$$

Therefore, comparing the Taylor series expansions of the relevant Hilbert series, up to a significant order (e.g., degree 8 or higher), provides strong evidence for or against a conjectured mirror symmetry relationship.

Chapter 4

Brane Dynamics

Having established the mathematical tools for identifying and verifying mirror symmetry, we now turn to its constructions. This chapter explores how $3d \mathcal{N} = 4$ quiver gauge theories, and the mirror symmetry they exhibit, can be understood as phenomena within Type IIB string theory. We will introduce the relevant brane configurations – D3, D5, and NS5-branes – and demonstrate their direct correspondence to the gauge groups, flavour symmetries, and matter content of quiver theories [8]. We will see how string theory dualities lead to a systematic algorithm for constructing mirror pairs from these brane setups.

4.1 Branes

We consider Type IIB string theory formulated in a ten-dimensional spacetime, comprising one time dimension, denoted x_0 , and nine spatial dimensions, (x_1, \dots, x_9) . Within this spacetime, branes are dynamical extended objects. A p -brane, by definition, extends across p spatial dimensions in addition to the time dimension x_0 . As it evolves temporally, a p -brane sweeps out a $(p+1)$ -dimensional subspace known as its worldvolume.

The Type IIB string theory engineered to realise $3d \mathcal{N} = 4$ gauge theories typically involves three types of branes:

- **NS5-branes:** These 'Neveu-Schwarz' 5-branes extend along the spatial dimensions $\{x_1, x_2, x_3, x_4, x_5\}$. They possess definite positions along the x_6 direction and $\vec{w} = (x_7, x_8, x_9)$.
- **D5-branes:** 'Dirichlet' 5-branes extend along spatial directions $\{x_1, x_2, x_7, x_8, x_9\}$. They are localised at specific positions along x_6 and $\vec{m} = (x_3, x_4, x_5)$.

- **D3-branes:** These branes extend along the spatial directions $\{x_1, x_2, x_6\}$. They maintain constant positions in the remaining directions. Crucially, D3-branes have finite extent along x_6 and must end on either NS5-branes or D5-branes. There are three configurations for suspending D3-branes:

- Between two distinct NS5-branes: In this case, the D3-brane segment is free to move within the \vec{m} direction.
- Between two distinct D5-branes: Here, the D3-brane segment can move within the \vec{w} direction.
- Between an NS5-brane and a D5-brane.

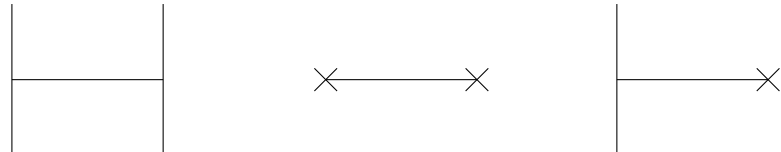
	x_0	x_1	x_2	x_3	x_4	x_5	x_6	x_7	x_8	x_9
D3	✓	✓	✓				✓			
D5	✓	✓					✓	✓	✓	✓
NS5	✓	✓	✓	✓	✓	✓		✓		

Table 4.1: Span of the spacetime dimensions of D3, D5 and NS5-branes.

The configuration involving NS5-branes and D5-branes is known to preserve precisely eight supercharges. Importantly, the introduction of D3-branes suspended between these 5-branes can be achieved without breaking any additional supersymmetry [8]. It is also pertinent to note the significant mass difference between these objects: the 5-branes are considerably heavier than the D3-branes.

Within this work, we will visualise these brane configurations adopt the convention that the spatial directions $\vec{w} = (x_7, x_8, x_9)$ will be represented by a vertical line; the x_6 direction will be represented by a horizontal line; and the directions $\vec{m} = (x_3, x_4, x_5)$ extending into the page will be indicated by a cross symbol.

Employing these conventions, the three distinct configurations for suspending D3-branes—between two NS5-branes (left), between two D5-branes (middle), or between an NS5-brane and a D5-brane (right) can be represented diagrammatically as follows.



4.2 Quiver Theories and Branes

Assuming all D3-branes end on NS5-branes, here is how we can construct $3d \mathcal{N} = 4$ theories from brane setups:

1. **Identify Intervals:** Each region between two adjacent NS5-branes defines an interval.
2. **Determine Gauge Groups:** For each interval, count the number of D3-branes, N_i , that extend across the interval. Then N_i defines a $U(N_i)$ gauge group associated with interval i . Represent each $U(N_i)$ gauge group as a circular node in the quiver diagram.
3. **Determine Flavor Groups:** For each interval, count the number of D5-branes, K_i , that are present within that interval. Then K_i corresponds to a flavour symmetry group associated with interval i . Represent this flavour symmetry by a square node labeled K_i .
4. **Determine Matter Fields:**
 - **Gauge-Gauge Connections:** Connect the gauge groups $U(N_i)$ and $U(N_{i+1})$ corresponding to adjacent intervals via an edge. This edge represents a hypermultiplet transforming in the bifundamental representation of $U(N_i) \times U(N_{i+1})$.
 - **Gauge-Flavor Connections:** Connect the gauge node $U(N_i)$ to the flavour node K_i (if $K_i > 0$) via an edge. This edge represents K_i hypermultiplets, each transforming in the fundamental representation of the $U(N_i)$ gauge group and the fundamental representation of the K_i flavour group.

Similarly, one can construct the brane setup from a quiver. We now address how the concept of $3d$ mirror symmetry manifests within this Type IIB framework.

4.3 3d Mirror Symmetry and Branes

In the context of the Type IIB brane system, the $3d$ mirror symmetry is realised through S -duality transformation. This duality acts by exchanging NS5-branes with D5-branes, while D3-branes remain unchanged. Consequently, a brane configuration

realising a specific $3d$ $\mathcal{N} = 4$ theory Q_1 is mapped under S-duality to its mirror dual theory Q_2 .

A necessary condition for self-mirror symmetry arises when the number of NS5-branes, n_s , equals the number of D5-branes, n_d [8]. For instance, in our quiver example in Chapter 3, there are 2 gauge nodes corresponding to 2 intervals separated by 3 NS5-branes, so $n_s = 3$ and the flavour node has colour 3, so $n_d = 3$. So the theory indeed might be self-mirrored.

Algorithm 1 *A systematic procedure exists within the brane setup to construct the mirror dual of a linear $3d$ $\mathcal{N} = 4$ theory. Beginning with the brane configuration representing the initial theory in the Coulomb branch, the steps are as follows [3]:*

1. **Move to the Origin:** Move the D3-branes are along the \vec{m} directions until their positions align with those of the D5-branes. This procedure corresponds to setting the VEVs associated with the Coulomb branch scalars to zero, thereby reaching the origin, $\langle \phi^V \rangle = 0$, of the moduli space where the Coulomb and Higgs branches intersect.
2. **Reconfigure D3-branes on D5-branes:** At the origin, the D3-branes can reconnect or break. Furthermore, the relative positions of the 5-branes can be rearranged according to the Hanany-Witten effect [7], [8]: when an NS5-brane and a D5-brane pass through each other, a D3-brane stretching between them is created (or annihilated). These two operations are repeated in an appropriate sequence until all D3-branes are suspended between pairs of D5-branes.
3. **Perform S-duality Transformation:** $NS5 \leftrightarrow D5$.
4. **Move onto the Higgs Branch:** Move the D3-branes away from the alignment points along the \vec{m} directions. This corresponds physically to activating VEVs for hypermultiplet scalars, effectively moving onto its Higgs branch.

The result can be confirmed using Hilbert series computations for the Higgs and Coulomb branches of both quivers in the pair. We can easily extend the construction above and show that the following family of quivers are self-mirrored.

$$\begin{array}{ccccccc} \circ & \text{---} & \circ & \cdots & \circ & \text{---} & \square \\ U(1) & & U(2) & & U(N-1) & & N \end{array}$$

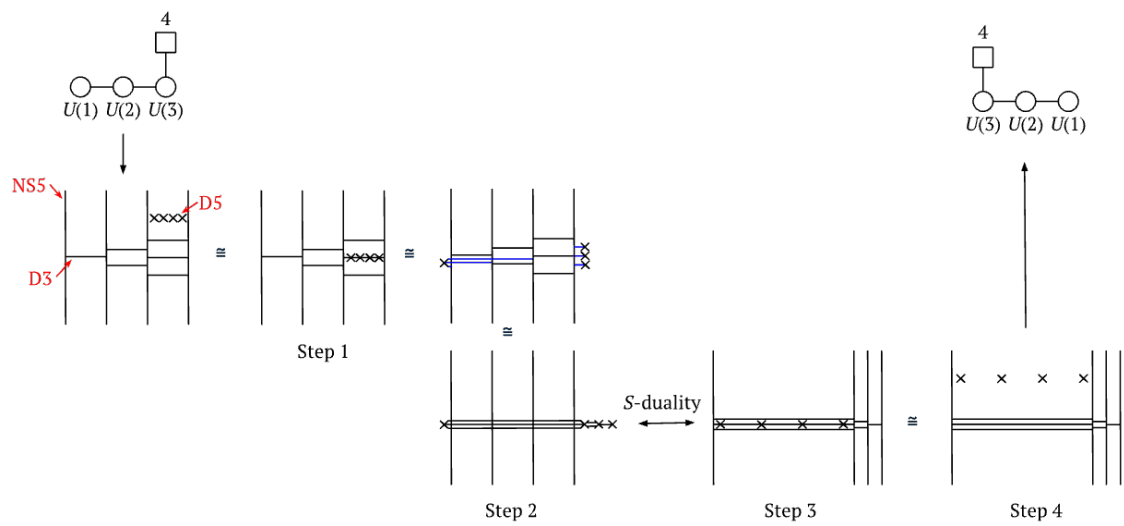


Figure 4.1: An example of 3d mirror symmetry construction via brane setups.

Chapter 5

Non-linear Quivers

Armed with all the background presented in the previous chapters—the theory, the analytical tools, and the physical intuition—this chapter now embarks on the central original contribution of this dissertation. We extend from the study of known mirror pairs to the exploration of new mirror pairs, specifically focusing on quiver geometries that extend beyond simple linear or ADE types. Here, we propose a novel infinite family of $3d$ mirror pairs, denoted $Q_{[n;\{g_i\};\{l_i\}]}$ and $P_{[n;\{g_i\};\{l_i\}]}$, for which we establish duality via a general inductive proof, its base case having been explicitly verified up to $n=6$ through Hilbert Series computations. These theories are characterised by Abelian $U(1)$ quiver diagrams exhibiting distinctive branched cyclic structures. This chapter will define these quiver families, articulate the mirror symmetry postulate in full detail, and present the complete evidence supporting this claim, encompassing the aforementioned Hilbert Series computations and the constructive inductive proof.

The motivation for examining this particular class extends beyond the specifics of these branched structures. By establishing and analysing the proposed duality for these non-linear, yet purely Abelian, quiver theories, we aim to cultivate a deeper understanding of the mechanisms underlying $3d$ mirror symmetry in contexts beyond the simpler geometries studied previously. It is hoped that the principles uncovered in this simpler, constrained setting may offer valuable insights and guidance for the future exploration of dualities involving more general, potentially non-Abelian, quiver gauge theories.

Throughout this chapter and the remainder of this work, the following conventions will be adopted for all quiver diagrams presented, unless explicitly specified otherwise:

- Circular nodes represent $U(1)$ gauge groups.
- Square nodes represent rank-1 flavour nodes.

- In instances where nodes are labelled with an integer k inside the node, a circular node denotes a $U(k)$ gauge group, while a square node signifies a rank- k flavour group.
- When depicting a quiver diagram that contains no explicit flavour nodes, it will be implicitly assumed that an overall $U(1)$ vector multiplet decouples from the theory.

We now state the central postulate regarding a novel infinite family of $3d$ mirror pairs.

5.1 The Postulate

Postulate 1 *We propose that for any integer $n \geq 3$, and associated sets of integers $\{g_1, \dots, g_n\}$ defining cyclic positions and $\{l_1, \dots, l_n\}$ defining ray lengths, which satisfy the constraints $0 < g_1 < g_2 < \dots < g_n$ and $\forall i \in \{1, \dots, n\}$, $l_i > 0$, the following two families of $3d$ $\mathcal{N} = 4$ quiver gauge theories, denoted $Q_{[n; \{g_i\}; \{l_i\}]}$ and $P_{[n; \{g_i\}; \{l_i\}]}$, constitute a mirror dual pair.*

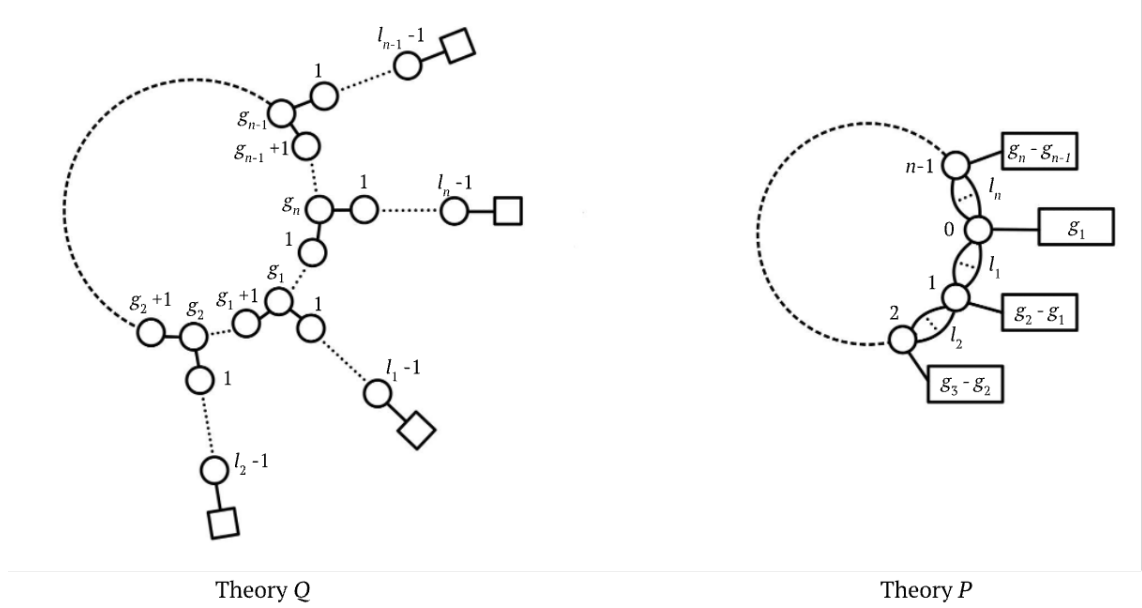


Figure 5.1: The $3d$ mirror pairs Theory $Q = Q_{[n; \{g_i\}; \{l_i\}]}$ and Theory $P = P_{[n; \{g_i\}; \{l_i\}]}$

The specific structures of these two families of theories are detailed below:

- The $Q = Q_{[n; \{g_i\}; \{l_i\}]}$ Theory:

This theory has a central ring comprising g_n distinct $U(1)$ gauge nodes. These ring nodes are connected sequentially via bifundamental hypermultiplets. Emanating from this central ring are n linear ‘rays’ of nodes, attached at the ring nodes indexed by the specified cyclic positions g_1, \dots, g_n . The i -th ray consists of a linear chain of $l_i - 1$ $U(1)$ gauge nodes. The first node of this ray connects directly to the ring node g_i , and the final $(l_i - 1)$ -th node of the ray terminates on a rank-1 flavour node.

- The $P = P_{[n; \{g_i\}; \{l_i\}]}$ Theory:

This theory possesses a central ring structure, consisting of precisely n distinct $U(1)$ gauge nodes. The connection between adjacent gauge nodes j and $j + 1$ on this ring (where $n + 1 \equiv 1$) is mediated by l_j parallel edges. Furthermore, each gauge node j situated on the ring is connected to an associated rank- N_j flavour node, with $N_j = l_j - l_{j-1}$, where we let $p_0 = 0$.

5.2 Essential Tools: Quiver Operations

To provide evidence for the proposed mirror symmetry postulate, particularly when employing an inductive approach, specific operations for quiver diagrams are required.

A standard operation involves the concept of fixing or removing a “centre of mass” degree of freedom, which corresponds physically to the gauging or ungauging of an overall $U(1)$ symmetry factor often associated with flavour nodes. This is typically known in literature as framing/unframing [1]. Such operations are generally understood not to alter the intrinsic geometry of the moduli space. Consistent with previous conventions, when analysing quiver diagrams devoid of explicit flavour nodes, it is implicitly assumed that an overall $U(1)$ vector multiplet has been decoupled from the interacting theory. We now detail two key procedures.

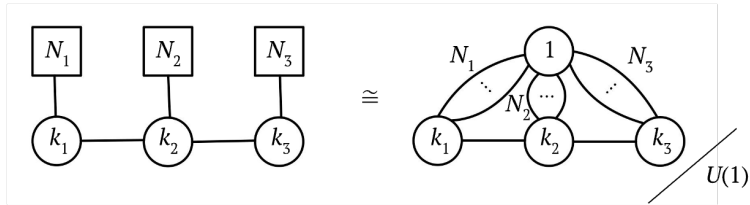


Figure 5.2: Fixing or removing a centre of mass preserves the moduli space

Fixing a Centre of Mass: Ungauging an Overall $U(1)$

This procedure transforms a $U(1)$ gauge symmetry into a global flavour symmetry. Physically, this corresponds to the associated $U(1)$ gauge boson acquiring an infinite mass, thereby fixing the centre of mass of the configuration. This operation assumes the initial quiver possesses no flavour nodes. The steps involved are:

1. Identify a target $U(1)$ gauge node intended for ungauging. Often, a node with a large number of edges is chosen. Remove the selected $U(1)$ gauge node from the quiver diagram.
2. For each gauge node that was previously connected to the removed $U(1)$ node via n edges, introduce a new rank- n flavour node and connect the original gauge node to this new flavour node with one edge representing these n hypermultiplets.

Removing the Centre of Mass: Gauging an Overall $U(1)$

Conversely, this procedure elevates a global $U(1)$ symmetry, typically associated with existing flavour nodes, to a local $U(1)$ gauge symmetry. The steps are as follows:

1. Begin with a quiver gauge theory that includes flavour nodes, denoted F_1, \dots, F_k , with respective ranks N_{F_1}, \dots, N_{F_k} .
2. Introduce a new $U(1)$ gauge node into the quiver diagram.
3. For each original flavour node F_i of rank N_{F_i} that was connected to an original gauge node (say, node i), connect the new $U(1)$ gauge node to the original gauge node i with N_{f_i} edges. Remove the original flavour nodes F_i .

Finally, we define a key operation utilised in constructing the postulated mirror quiver theories, we will call it **Flavour-Gauged Linking operation**, along with its corresponding transformation under $3d$ mirror symmetry. This operation will allow us to find new mirror pairs starting with a known mirror pair [6].

The procedure involves two initial theories with all rank-1 nodes: a general quiver, denoted Q_1 , and a linear quiver, Q_2 , with two rank-1 flavour nodes attached at each end of the linear gauge nodes. The operation proceeds by identifying a rank-1 flavour node F_1 of a general quiver Q_1 with a rank-1 flavour node F_2 of a linear quiver Q_2 . Subsequently, the unified $U(1)$ flavour symmetry associated with the identified node ($F_1 \equiv F_2$) is gauged, promoting it to a local $U(1)$ gauge symmetry within the composite theory constructed from Q_1 and Q_2 .

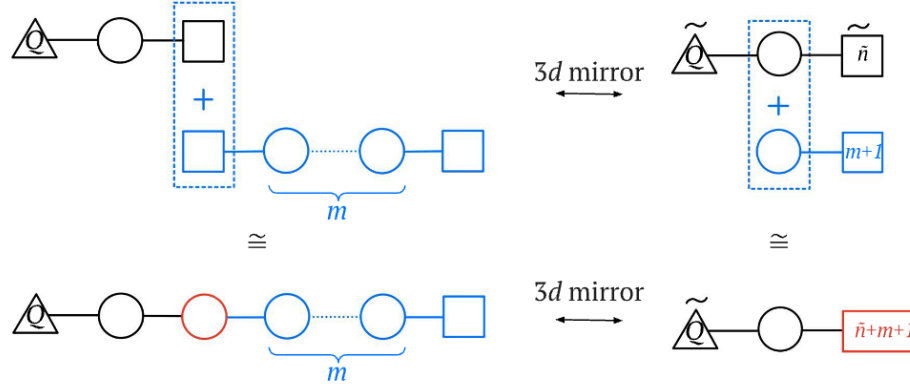


Figure 5.3: Flavour-Gauged Linking operation (left) and its corresponding mirror operation (right)

We will prove this is indeed the mirror operation for the Flavour-Gauged Linking operation when Q_1 is a general linear quiver via a brane setup. For a linear quiver Q_1 with k $U(1)$ gauge nodes and associated rank-1 flavour nodes with flavour $\forall i \in 1, \dots, k$, $N_i \in \{0, 1\}$ and Q_2 with m $U(1)$ gauge nodes.

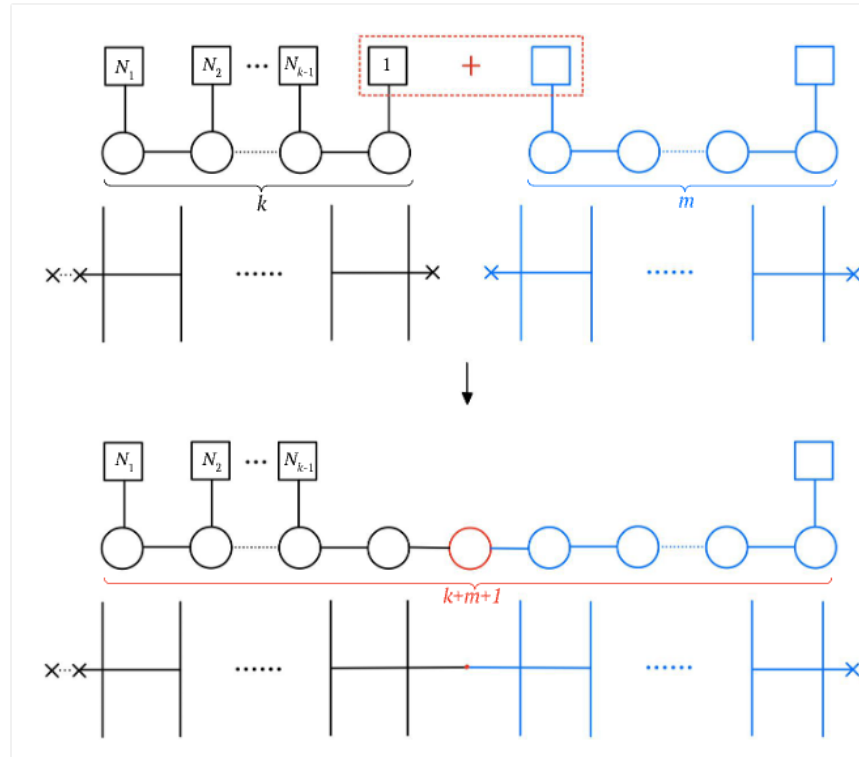


Figure 5.4: Brane setup of a general linear rank-1 quiver under Flavour-Gauged Linking operation

The initial step involves constructing the Type IIB brane configurations that realise theories Q_1 and Q_2 independently, followed by reconfiguring D3-branes onto D5-branes (Steps 1 and 2 of Algorithm 1). The Flavour-Gauged Linking operation then proceeds by identifying a specific rank-1 flavour node from Q_1 with one from Q_2 , followed by gauging the resulting unified $U(1)$ flavour symmetry. In the Figure 5.4, this corresponds to manipulating the D5-branes associated with these flavour nodes. Specifically, the identification and subsequent gauging translate to bringing together and merging the two D5-branes representing the identified flavour nodes, resulting in a unified brane configuration for the linked theory.

To ascertain the mirror operation, the S-duality transformation (exchanging NS5 \leftrightarrow D5) is applied to this resulting brane configuration. The number of NS5-branes in the original configuration is added, which become D5-branes after S-duality, corresponding to adding the rank of flavour nodes, consistent with Figure 5.3 right.

5.3 Verification of the Postulate

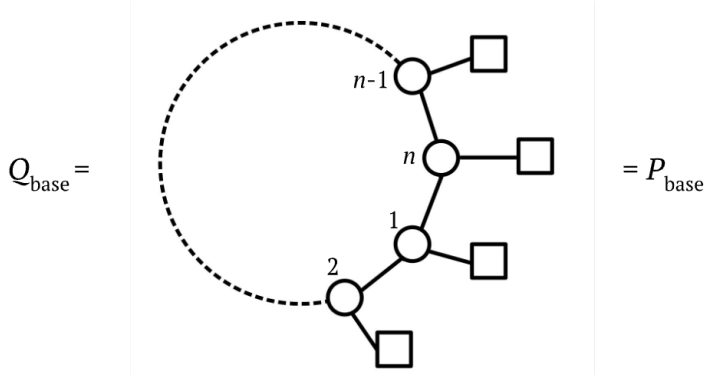
Building on the postulate introduced previously, which conjectures a mirror symmetry relationship between the $Q_{[n; \{g_i\}; \{l_i\}]}$ and $P_{[n; \{g_i\}; \{l_i\}]}$ families of theories, this section provide evidence for this duality. The approach combines direct verification for a base case using Hilbert Series calculations with an inductive argument designed to extend the result to general parameters $\{g_i\}$, and $\{l_i\}$ for each n .

Since the specific labelling of nodes and rays is arbitrary up to cyclic permutations and relabelling, the arguments can be made without loss of generality (WLOG) by induction on g_1 and l_1 .

5.3.1 Base Case Verification via Hilbert Series

The first step is to establish the validity of the postulate for the base cases. For each integer $n \geq 3$, we select the simplest non-trivial instance of the parameters: the cyclic positions are taken sequentially, $g_1 = 1, g_2 = 2, \dots, g_n = n$, and the ray lengths are set to their minimal values, $l_1 = l_2 = \dots = l_n = 1$. Let these base case theories be denoted Q_{base} and P_{base} .

We will verify the isomorphism between the respective moduli spaces, specifically $\text{Coulomb}(Q_{\text{base}}) \cong \text{Higgs}(P_{\text{base}})$ and $\text{Higgs}(Q_{\text{base}}) \cong \text{Coulomb}(P_{\text{base}})$ by comparing the Hilbert Series for the Coulomb and Higgs branches of both Q_{base} and P_{base} . Explicit computations performed for $n = 3, 4, 5, 6$ are presented in Appendix A. This demonstrates the expected result that Q_{base} and P_{base} are 3d mirror pairs.



Extending this direct verification via Hilbert Series computation to $n > 6$ faces significant computational challenges, primarily due to the complexity involved in evaluating the Monopole Formula for the Coulomb branch as the number of gauge nodes increases. Despite this computational limitation, the inductive argument is constructed to hold generally for all $n \geq 3$ provided the initial base cases are satisfied.

5.3.2 Inductive Argument

To extend the duality beyond the base case, we propose an inductive path leveraging the quiver manipulation tools discussed previously. The inductive hypothesis assumes that the mirror symmetry duality holds for a given set of valid parameters $[n; \{g_i\}; \{l_i\}]$. The induction proceeds in two main stages :

1. First Induction on ray lengths l_i : WLOG, we demonstrate that if the duality holds for parameters $\{l_1, \dots, l_n\}$, it also holds for $\{l_1 + 1, l_2, \dots, l_n\}$. Increasing l_1 by one corresponds, in the Q theory, to extending the first ray by Flavour-Gauged Linking a free hypermultiplet to the terminal flavour node. Applying the corresponding Mirror Operation to the mirror theory $P_{[n; \{g_i\}; \{l_i\}]}$ yield the proposed mirror pair $P_{[n; \{g_i\}; \{l_1 + 1, l_2, \dots, l_n\}]}$. Figure 5.5 completes the inductive step for the ray lengths l_i .
2. Second Induction on cyclic positions g_i : We demonstrate that if the duality holds for parameters $\{g_1, \dots, g_n\}$, it also holds for $\{g_1, g_2, \dots, g_n + 1\}$. To achieve this transformation, we first "unframe" the quiver, then ungauge the node $g_n - 1$. Then the Flavour-Gauged Linking operation is performed, linking the modified Q theory with a free hypermultiplet quiver at the newly created flavour node corresponding to the original $g_n - 1$ position. The mirror of this sequence of operations is applied to the P theory. Figure 5.6 completes the inductive step for the ring position g_n .

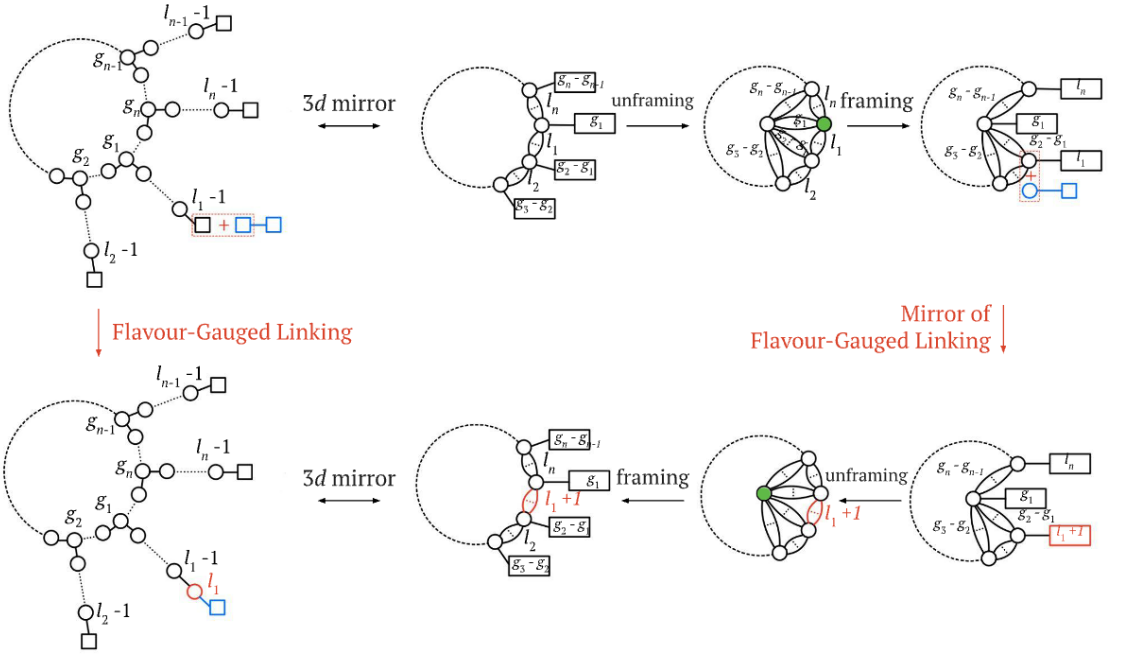


Figure 5.5: Proof by induction on parametre l_1

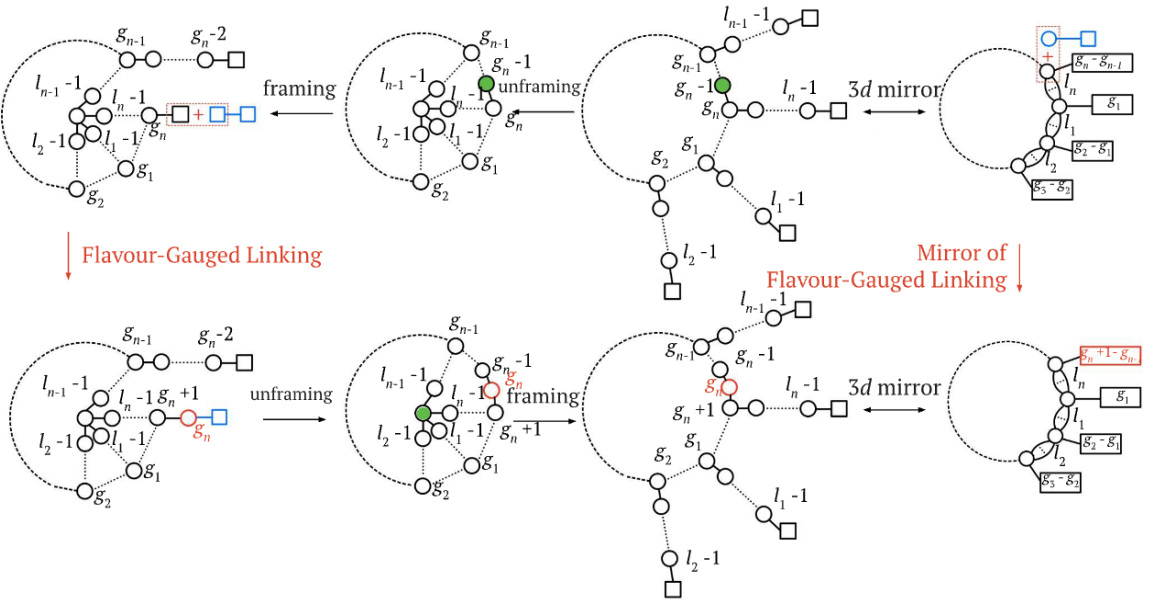


Figure 5.6: Proof by induction on parametre g_n

Further verification of the proposed mirror symmetry for the base case configurations was performed for specific small values of n .

For the case $n = 3$, the resulting Hilbert series and inferred moduli space structures were compared with established results in the literature [5]. Our findings are fully consistent with the properties described for "Family II" in the paper Three Dimensional Mirror Symmetry beyond ADE quivers and Argyres-Douglas theories, under an appropriate framing/unframing operation and change of parameters between the two notions.

For $n = 4$, explicit computations of the relevant Hilbert Series were carried out for the first few distinct quiver structures. The complete results of these computations are in Appendix B. Together, these explicit checks for $n = 3$ and $n = 4$ provide substantial evidence validating the proposed mirror duality for these foundational configurations.

In summary, this chapter has proposed a new infinite family of $3d \mathcal{N} = 4$ mirror pairs, $Q_{[n; \{g_i\}; \{l_i\}]}$ and $P_{[n; \{g_i\}; \{l_i\}]}$ characterised by Abelian quivers with branched cyclic structures, thereby extending the known scope of mirror symmetry beyond linear or ADE geometries. Evidence supporting this postulate was provided through explicit Hilbert Series computations verifying a base case, alongside a constructive inductive argument founded on the Flavour-Gauged Linking operation and its established mirror counterpart.

This postulated duality involving branched Abelian quivers opens several promising avenues for future research. Notably, exploring potential generalisations of these branched structures and their associated dualities to incorporate non-Abelian gauge groups remains an important direction for expanding our understanding of the supersymmetric gauge theory dualities and their association to the Lagrangian.

Bibliography

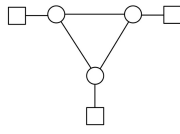
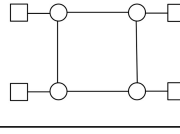
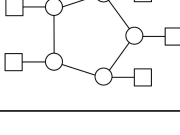
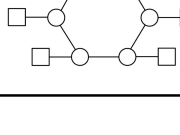
- [1] Luis F. Alday, Davide Gaiotto, and Yuji Tachikawa. Liouville correlation functions from four-dimensional gauge theories. 91(2):167–197.
- [2] P. C. Argyres, M. R. Plesser, and N. Seiberg. The moduli space of n=2 SUSY QCD and duality in n=1 SUSY QCD. 471(1):159–194.
- [3] Antoine Bourget, Julius F. Grimminger, Amihay Hanany, Rudolph Kalveks, and Zhenghao Zhong. Higgs branches of u/SU quivers via brane locking. 2022(8):61.
- [4] Stefano Cremonesi, Amihay Hanany, and Alberto Zaffaroni. Monopole operators and hilbert series of coulomb branches of 3d n = 4 gauge theories. 2014(1):5.
- [5] Anindya Dey. Three dimensional mirror symmetry beyond \$ADE\$ quivers and argyres-douglas theories. 2021(7):199.
- [6] Anindya Dey, Amihay Hanany, Peter Koroteev, and Noppadol Mekareeya. Mirror symmetry in three dimensions via gauged linear quivers. 2014(6):59.
- [7] Davide Gaiotto and Edward Witten. S-duality of boundary conditions in n=4 super yang-mills theory. 13(3):721–896.
- [8] Amihay Hanany and Edward Witten. Type IIB superstrings, BPS monopoles, and three-dimensional gauge dynamics. 492(1):152–190.
- [9] K. Intriligator and N. Seiberg. Mirror symmetry in three dimensional gauge theories. 387(3):513–519.

Appendix A

Hilbert Series Verification for Base Cases

This table shows the Hilbert Series computations verifying the mirror symmetry postulate for the defined base cases for $n = 3, 4, 5, 6$.

Table A.1: Hilbert Series base case computation for $n = 3, 4, 5, 6$

Parametre	Theory $Q_{\text{base}} = P_{\text{base}}$	Hilbert Series
$n = 3$		$\text{HS}_C = 1 + 3t^2 + 8t^3 + 12t^4 + 24t^5 + 48t^6 + 72t^7 + 117t^8 = \text{HS}_H$
$n = 4$		$\text{HS}_C = 1 + 4t^2 + 8t^3 + 20t^4 + 40t^5 + 84t^6 + 152t^7 + 285t^8 = \text{HS}_H$
$n = 5$		$\text{HS}_C = 1 + 5t^2 + 10t^3 + 25t^4 + 62t^5 + 135t^6 + 270t^7 + 550t^8 = \text{HS}_H$
$n = 6$		$\text{HS}_C = 1 + 6t^2 + 12t^3 + 33t^4 + 84t^5 + 202t^6 + 432t^7 + 942t^8 = \text{HS}_H$

Appendix B

Hilbert Series Computations for $n = 4$

This table demonstrates the resulting Hilbert Series computation for both Coulomb and Higgs branch for the first few set of parameters in a $n = 4$ theory, providing further proof of our Postulate 1.

Table B.1: Hilbert Series computation for first few $\{g_i\}$

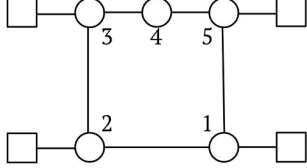
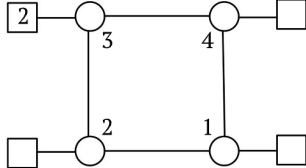
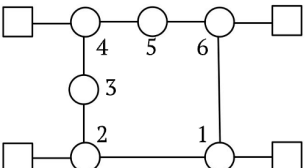
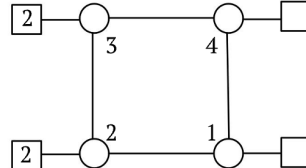
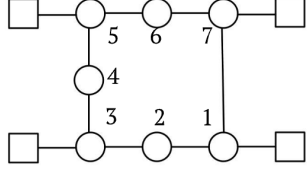
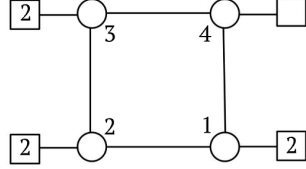
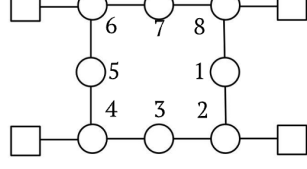
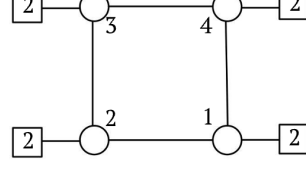
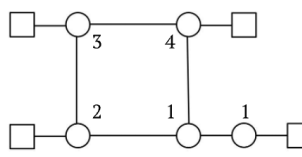
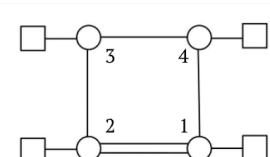
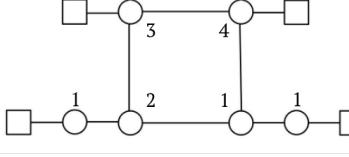
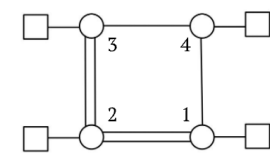
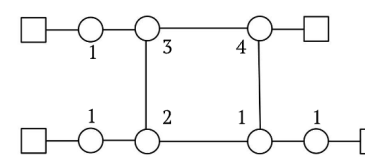
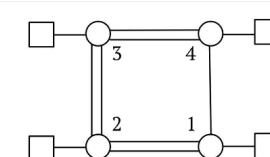
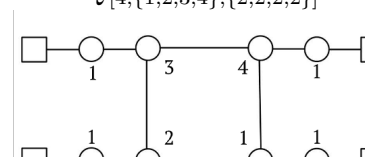
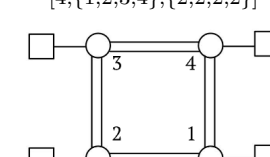
Theory Q	Theory P
$Q_{[4,\{1,2,3,5\},\{1,1,1,1\}]}$	$P_{[4,\{1,2,3,5\},\{1,1,1,1\}]}$
	
$HS_C = 1 + 7t^2 + 12t^3 + 41t^4 + 88t^5 + 215t^6 + 428t^7 + 902t^8 = HS_H$	
$HS_H = 1 + 4t^2 + 6t^3 + 16t^4 + 32t^5 + 64t^6 + 112t^7 + 209t^8 = HS_C$	
$Q_{[4,\{1,2,4,6\},\{1,1,1,1\}]}$	$P_{[4,\{1,2,4,6\},\{1,1,1,1\}]}$
	
$HS_C = 1 + 10t^2 + 18t^3 + 71t^4 + 174t^5 + 460t^6 + 1040t^7 + 2366t^8 = HS_H$	
$HS_H = 1 + 4t^2 + 4t^3 + 16t^4 + 20t^5 + 58t^6 + 76t^7 + 171t^8 = HS_C$	
$Q_{[4,\{1,3,5,7\},\{1,1,1,1\}]}$	$P_{[4,\{1,3,5,7\},\{1,1,1,1\}]}$
	
$HS_C = 1 + 13t^2 + 24t^3 + 114t^4 + 296t^5 + 882t^6 + 2168t^7 + 5424t^8 = HS_H$	
$HS_H = 1 + 4t^2 + 2t^3 + 16t^4 + 12t^5 + 50t^6 + 52t^7 + 139t^8 = HS_C$	
$Q_{[4,\{2,4,6,8\},\{1,1,1,1\}]}$	$P_{[4,\{2,4,6,8\},\{1,1,1,1\}]}$
	
$HS_C = 1 + 16t^2 + 32t^3 + 166t^4 + 480t^5 + 1528t^6 + 4160t^7 + 11144t^8 = HS_H$	
$HS_H = 1 + 4t^2 + 18t^4 + 60t^6 + 181t^8 = HS_C$	

Table B.2: Hilbert Series computation for first few $\{l_i\}$

Theory Q	Theory P
$Q_{[4,\{1,2,3,4\},\{2,1,1,1\}]}$ 	$P_{[4,\{1,2,3,4\},\{2,1,1,1\}]}$ 
$HS_C = 1 + 7t^2 + 10t^3 + 43t^4 + 80t^5 + 213t^6 + 406t^7 + 884t^8 = HS_H$ $HS_H = 1 + 4t^2 + 4t^3 + 20t^4 + 24t^5 + 70t^6 + 96t^7 + 221t^8 = HS_C$	
$Q_{[4,\{1,2,3,4\},\{2,2,1,1\}]}$ 	$P_{[4,\{1,2,3,4\},\{2,2,1,1\}]}$ 
$HS_C = 1 + 10t^2 + 12t^3 + 79t^4 + 136t^5 + 470t^6 + 900t^7 + 2324t^8 = HS_H$ $HS_H = 1 + 4t^2 + 16t^4 + 10t^5 + 48t^6 + 44t^7 + 127t^8 = HS_C$	
$Q_{[4,\{1,2,3,4\},\{2,2,2,1\}]}$ 	$P_{[4,\{1,2,3,4\},\{2,2,2,1\}]}$ 
$HS_C = 1 + 13t^2 + 14t^3 + 128t^4 + 210t^5 + 916t^6 + 1748t^7 + 5344t^8 = HS_H$ $HS_H = 1 + 4t^2 + 12t^4 + 10t^5 + 34t^6 + 44t^7 + 85t^8 = HS_C$	
$Q_{[4,\{1,2,3,4\},\{2,2,2,2\}]}$ 	$P_{[4,\{1,2,3,4\},\{2,2,2,2\}]}$ 
$HS_C = 1 + 16t^2 + 16t^3 + 196t^4 + 304t^5 + 1672t^6 + 3120t^7 + 11380t^8 = HS_H$ $HS_H = 1 + 4t^2 + 10t^4 + 8t^5 + 26t^6 + 38t^7 + 65t^8 = HS_C$	